Second-order sloshing over an arbitrary bed

By G. J. D. CHAPMAN AND R. PORTER

School of Mathematics, University of Bristol, BS8 1TW, UK

The two-dimensional problem of the free sloshing of an inviscid fluid in a vertically-walled tank with an arbitrary bed shape is solved at both first and second-order in the Stokes expansion of the velocity potential. The approach employed at both orders uses Green's functions for a flat-bed in conjunction with the Cauchy-Riemann equations to derive integral equations for the tangential flux along the varying bed. The first and second-order potentials everywhere in the fluid may then be related to these fluxes. Significant analytic progress is made with the calculation of various contributions to the integral equations at second order. The equations at first and second-order are ultimately solved using a variational principle equivalent to the Galerkin method giving efficient and accurate results. In particular, the work involved in determining the second-order solution is no more intensive than solving the first-order problem. The first-order solution is shown to reproduce known results for specific bed shapes. The method is applied to a range of bed shapes and the second-order correction to the free-surface elevation is illustrated.

1. Introduction

The sloshing problem is a classical eigenvalue problem of fluid mechanics, a standard reference for which is Lamb (1932). The references in Lamb show the problem's long history and the illustrious names involved with it; however, he notes that despite such long standing attention, the number of cases of motion with a variable depth for which the solution has been obtained is very small. Lamb presents the analysis for a triangular canal whose section consists of two straight lines inclined at $\pi/4$ to the vertical and which, to date remains one of the few cases for which an analytical solution is known. During the mid-twentieth century there was an upsurge of interest in the sloshing problem driven by the need to develop a theory of the motion of fluid within partially filled containers. The main applications of the era as highlighted by Moiseev (1964) were all aspects of fuel tank problems, ranging from aircraft fuel within wings to liquid fuelled rockets, as well as, for example, seismic oscillations of structures under water pressure. Moiseev (1964) and subsequently Moiseev & Petrov (1968) provided extensive reviews of the linear theory and main references of the period. Although Moiseev states that most of the applications occur in circumstances where perturbation theory proves extremely effective, he reiterates that even the linearised case calls for numerical calculation. Moiseev does not deal with non-linear oscillations where he states that many of the algorithms of the time were clumsy and convergence was unproved.

The advent of high-power computational facilities has enabled researchers to make progress, albeit numerically, in the sloshing problem. The motivation is still driven by the technological problems arising from the often violent motion of the fluid within partially-filled fluid containers. Efficient and accurate calculation of sloshing frequencies remains

an important goal as it is desirable to avoid the resonance which is known to occur in a system externally forced at, or near, a sloshing frequency. It is also known that violent motions can induce large pressures so accurate modelling of the motion is also required to estimate the pressures and to engineer safe containers. Research has continued actively in two complementary directions, namely identifying the sloshing frequencies, and modelling the non-linear fluid motion.

There has been much work on non-linear sloshing motions based on improving modal approaches or using computational fluid dynamics code. Some papers are discussed below and the references therein provide a fair coverage of the field. Faltinsen (1974) found analytic results for the motion of a two-dimensional rectangular tank forced to oscillate harmonically at frequencies close to the lowest natural mode of oscillation and with small amplitudes of roll or sway. Faltinsen, Rognebakke, Lukovsky & Timokha (2000), Faltinsen & Timokha (2001), Faltinsen & Timokha (2002) and Faltinsen, Rognebakke & Timokha (2002) develop a multi-dimensional modal approach using generalised domain and surface modes rather than natural modes. This basic approach, and its refinements in the later papers as they develop are shown to model sloshing in intermediate to small depths and in tanks where the length to breadth ratio is $O(1)$ and therefore a two-dimensional approach is questionable. However, they note the difficulties inherent in a modal approach of dealing with run-up, overturning and dissipation due to local breaking. The sloshing problem is also amenable to non-linear solvers, for example see Wu & Eatock Taylor (1994) who apply their finite-element method code to consider the sloshing problem in a rectangular tank. Their approach is to perform a finite-element analysis, obtaining the solution through a variational principle and obtaining the fluid motion by a Galerkin approach. They extend this work in Wu & Eatock Taylor (1998) where they consider three-dimensional translational motion in a rectangular tank and observe travelling waves and bores in addition to standing waves. Their work is calibrated by checking that their three-dimensional code applied to two-dimensional motion gives consistent results with two-dimensional solvers. In the course of this paper they clearly demonstrate that there remain many interesting problems associated with the sloshing problem.

The other main direction of research has focussed on the calculation of linear sloshing frequencies. Davis (1965) established important results regarding uniqueness of solution and provided asymptotics of the eigenvalues for two-dimensional oscillations in canals of arbitrary cross section. In Davis (1974) significant progress was made in asymptotics for the semi-circular cross section which at the time remained unsolved. Packham (1980) solved the case for a triangular canal with sides inclined at $\pi/6$ to the horizontal. Craggs & Duck (1978) show how techniques from complex-variable theory may be applied to two-dimensional problems and proceed to solve the segmental and arbitrary triangular cross section. Fox & Kuttler (1983) provide an extensive review of the two-dimensional sloshing problem and appropriate references. In their paper they provide upper and lower bounds for numerous cross sections by using conformal mappings from the specific geometry to one whose explicit solution is known. They also refer to a series of papers by Henrici, Troesch & Wuytack (1970), Troesch & Troesch (1972), Miles (1972), Troesch (1973) and Troesch (1972) on the 'ice-fishing' problem, or sloshing in a strip aperture in an infinite half-space. This is important in providing bounds on sloshing frequencies through domain monoticity, meaning that if two domains have the same free-surface but one domain contains the other then the containing region has the larger sloshing frequency. This theoretical result is also confirmed in the numerical results we produce in the present paper. Later work by McIver (1989) has looked at cylindrical and spherical containers

filled to arbitrary depths. Evans & Linton (1991) also considered both an infinite and finite cylinder with semi-circular cross section as well as a hemisphere, and presented an extremely efficient technique of calculating the lowest sloshing frequencies.

Despite the long history of the sloshing problem, there is relatively little work on the case of arbitrary bed shapes. The Mild-Slope Equation (MSE), often attributed to Berkhoff (1973), and later refinements by Chamberlain & Porter (1995) (Modified Mild-Slope Equations - MMSE) introduce approximate analytical techniques essentially involving depth-averaging under the assumption of small variations in the bed shape. The MSE/MMSE prove to be very effective at solving problems involving, for example, Bragg resonance and scattering by arbitrary bed profiles, see, for example, Porter & Porter (2003). Booij (1983) has used the MSE to compute oblique sloshing in a tank with a flat sloping bottom and appeared to obtain quite good agreement with a numerical solution based on a finite-element method. More recently Belibassakis & Athanassoulis (2002) have demonstrated an extension of the MSE which deals with variable bed profiles by expanding in terms of a complete set of depth modes for the flat bottom and adding in a function to ensure the arbitrary profile's boundary condition is met.

The focus of this paper is on solving the sloshing problem to second-order providing a weakly non-linear solution. Essentially this introduces the much more complicated free-surface problem whereby the first-order potential forces the second-order potential, in essence having the effect of a pressure distribution on the free-surface in the second-order problem. Wehausen & Laitone (1960) §21 discuss this problem in general, whereas later papers on second-order scattering such as Vada (1987), McIver & McIver (1990) and McIver (1994) make use of the specific form of this forcing to solve scattering problems.

We base our approach on the Green's Identity method of Porter & Porter (2000) and, through careful formulation and manipulation, we are able to extend it to the much more complicated second-order problem. Fundamental to this is the use of the Cauchy-Riemann equations to convert normal to tangential derivatives simplifying the integral equations to be solved. It should be emphasised that our formulation is *exact* at each order, satisfying the no-flow condition at the bed and the complicated free-surface boundary conditions. We show how to apply the approach twice, non-trivially dealing with the problem of defining the first order potential on the free-surface, which is required to feed into the second-order problem. This key step to our problem did not need to be calculated in Porter & Porter to determine the scattering coefficients and was therefore not considered. The second-order problem requires more careful manipulation as, in this case, the integral equation to be solved is inhomogeneous. However, we find it is possible to solve it and find a solution expressed in terms of the coefficients of the first-order solution. We formulate the problem and then proceed to solve at first-order showing how to calculate the sloshing frequencies and how to obtain an expression for the first-order potential. We then show how to solve the second-order problem, again yielding solutions for the second-order potential on the free-surface which is required to calculate the free-surface elevation. We present calculations of the sloshing frequencies confirming that our method gives correct results for known bed shapes. We also compare our results for sloshing frequencies with those predicted by the MSE and MMSE and present results showing that, for the sloshing problem at least, the MSE/MMSE's effectiveness not only depends upon the maximum slope but on the specific geometry under consideration. Although our formulation is exact, the Galerkin approximation used to solve the integral equations provides an approximate solution at first-order, so we present data indicating the rapid convergence of the approximation. Finally we show the second-order corrections to the first order surface elevations.

2. Formulation and preliminaries

We consider surface gravity waves upon a fluid which is assumed to be incompressible and inviscid, and whose motion is irrotational. The fluid motion, which is taken to be two-dimensional, may therefore be described in terms of a velocity potential $\Phi(x, y, t)$ which satisfies Laplace's equation in the domain occupied by the fluid. Here x is the horizontal axis and y is the vertical axis (positive downwards), with $y = 0$ representing the undisturbed free-surface. We choose the wave steepness ε as the small parameter of the problem and so may expand the velocity potential and wave elevation as

$$\begin{aligned} \Phi &= \varepsilon\Phi_1 + \varepsilon^2\Phi_2 + O(\varepsilon^3), \\ \eta &= \varepsilon\eta_1 + \varepsilon^2\eta_2 + O(\varepsilon^3). \end{aligned} \tag{2.1}$$

The derivation of the equations to be satisfied at first, second and higher orders of this expansion is well known and so will not be repeated here. See, for example Mei (1983) who gives an elegant scaling argument to deduce wave steepness as the small parameter, and, although he only derives the linearised equations, this argument may be continued to higher orders. The scaling argument applied to higher orders also yields the additional requirement, highlighted in Stokes (1847), of short waves/deep water for the small parameter expansion to remain valid.

The problem is to determine the sloshing modes in a tank whose walls are at $x = 0, x = l$ and whose bed is given by the curve C defined as $y = h(x)$. We define the constant depth d such that $d = \max\{h(x) | x \in [0, l]\}$. The tank walls and bed are impermeable so the fluid velocity normal to these fixed boundaries is zero. In this case the equations to be satisfied by Φ_1 and Φ_2 are

$$\nabla^2 \Phi_i = 0, \qquad (x, y) \in D, \tag{2.2}$$

$$\frac{\partial \Phi_i}{\partial n} = 0, \qquad y = h(x),\ 0 < x < l, \tag{2.3}$$

$$\frac{\partial \Phi_i}{\partial x} = 0, \qquad \text{on } \{x = 0,\ 0 < y < h(0)\} \cup \{x = l,\ 0 < y < h(l)\}, \tag{2.4}$$

for $i = 1, 2$, where $\partial/\partial n \equiv \mathbf{n}.\nabla$ with $\mathbf{n}$ as the unit outward normal on C, and D is the region occupied by the fluid. The kinematic and dynamic free-surface boundary conditions combine, upon eliminating the dependence on η_1, η_2, to give

$$\frac{\partial^2 \Phi_1}{\partial t^2} - g\frac{\partial \Phi_1}{\partial y} = 0, \qquad \text{on } y = 0 \tag{2.5}$$

at first order and

$$\frac{\partial^2 \Phi_2}{\partial t^2} - g\frac{\partial \Phi_2}{\partial y} = -\frac{\partial}{\partial t}\left[(\nabla\Phi_1)^2\right] - \frac{1}{g}\frac{\partial \Phi_1}{\partial t}\frac{\partial}{\partial y}\left[\frac{\partial^2 \Phi_1}{\partial t^2} - g\frac{\partial \Phi_1}{\partial y}\right], \qquad \text{on } y = 0 \tag{2.6}$$

at second-order (see, for example, McIver & McIver (1990)). The first and second-order surface elevations are recovered from the expressions

$$\eta_1 = \text{Re}\left\{\frac{1}{g}\frac{\partial \Phi_1}{\partial t}\right\}, \qquad \text{on } y = 0 \tag{2.7}$$

and

$$\eta_2 = \frac{1}{g}\left(\frac{\partial \Phi_2}{\partial t} + \eta_1\frac{\partial^2 \Phi_1}{\partial y\partial t} + \frac{1}{2}(\nabla\Phi_1)^2\right), \qquad \text{on } y = 0 \tag{2.8}$$

Assuming time harmonic motion of frequency ω for the first-order potential we write

$$\Phi_1(x, y, t; K) = \text{Re}\left\{\phi_1(x, y; K)e^{-i\omega t}\right\} \tag{2.9}$$

where the frequency parameter is

$$K = \frac{\omega^2}{g}. \tag{2.10}$$

The time-independent first-order potential now satisfies

$$
\begin{aligned}
\nabla^2 \phi_1 &= 0, & (x, y) &\in D, \\
\frac{\partial \phi_1}{\partial y} + K\phi_1 &= 0, & \text{on } y &= 0, \ 0 < x < l, \\
\frac{\partial \phi_1}{\partial x} &= 0, & \text{on } \{x = 0, \ 0 < y < h(0)\} &\cup \{x = l, \ 0 < y < h(l)\}, \\
\frac{\partial \phi_1}{\partial n} &= 0, & \text{on } y &= h(x), \ 0 < x < l.
\end{aligned}
\tag{2.11}
$$

In the case of constant depth $h(x) = d$ this problem is easily solved by separation of variables to give modal solutions

$$\phi_1^{(n)} = C_n \cos \mu_n x \cosh \mu_n (y - d) \tag{2.12}$$

for arbitrary coefficients C_n where

$$\mu_n = \frac{n\pi}{l} \qquad n = 1, 2, \dots. \tag{2.13}$$

with frequencies $\omega = \omega_n$ determined by the dispersion relation

$$K = \mu_n \tanh(\mu_n d). \tag{2.14}$$

So for the first mode, for example, the dimensionless wavenumber $\mu_n l$ is given by π which, for a tank where $l/d = 1$ gives a dimensionless frequency $Kl = 3.1299$, and for a tank where $l/d = 2$, gives $Kl = 2.8813$.

We also follow Vada (1987) and McIver & McIver (1990) to express the second-order free-surface boundary condition as

$$\frac{\partial^2 \Phi_2}{\partial t^2} - g\frac{\partial \Phi_2}{\partial y} = \text{Re}[F(x)e^{-2i\omega t}] + F_s(x), \qquad \text{on } y = 0 \tag{2.15}$$

where

$$F(x) = \left[i\omega(\nabla\phi_1)^2 - \tfrac{1}{2}i\omega\phi_1\frac{\partial}{\partial y}\left(K\phi_1 + \frac{\partial \phi_1}{\partial y}\right) \right]_{y=0} \tag{2.16}$$

and

$$F_s(x) = \frac{i\omega}{4}\left[\phi_1\overline{\frac{\partial^2 \phi_1}{\partial x^2}} - \overline{\phi_1}\frac{\partial^2 \phi_1}{\partial x^2} \right]_{y=0} \tag{2.17}$$

and $\overline{\phi}$ denotes the complex conjugate of ϕ.

In the solution to both the first and second-order problem we will make use of the Green's function for a two-dimensional infinite domain with a constant depth d which we will denote $G_1(x, y | x_0, y_0)$, and which satisfies

$$
\left.
\begin{aligned}
\nabla^2 G_1 &= -\delta(x - x_0)\delta(y - y_0), & -\infty < x < \infty, \ 0 < y < d, \\
\frac{\partial G_1}{\partial y} + KG_1 &= 0, & \text{on } y = 0, \\
\frac{\partial G_1}{\partial y} &= 0, & \text{on } y = d, \ -\infty < x < \infty \, .
\end{aligned}
\right\}
\tag{2.18}
$$

It has the form

$$G_1(x, y | x_0, y_0) = \sum_{n=0}^{\infty} \frac{\psi_n(y)\psi_n(y_0)}{2k_n d} \mathrm{e}^{-k_n|x-x_0|}, \tag{2.19}$$

where

$$\left. \begin{array}{rcl} \psi_n(y) & = & N_n^{-1/2} \cos k_n(d-y), \\ N_n & = & \frac{1}{2}\{1 + \sin(2k_n d)/2k_n d\}, \end{array} \right\} \quad n = 0, 1, 2, \ldots \tag{2.20}$$

and we have used $k_n \ (n = 1, 2, \ldots)$ to denote the positive real roots of

$$K = -k_n \tan k_n d$$

incorporating $k_0 = -\mathrm{i}k$ where k is the real root of the dispersion relation

$$K = k \tanh kd.$$

A derivation of this Green's function is presented in Mei (1983) however, it should be noted that the final expression therein contains a sign error.

We now construct, using the method of images, a Green's function $G(x, y | x_0, y_0; K)$ for the tank satisfying (2.18) for $0 < x < l$ with $G_x = 0$ on $x = 0, l$ for $0 < y < d$. Hence

$$G(x, y | x_0, y_0) = \sum_{m=-\infty}^{\infty} \{G_1(2ml + x, y | x_0, y_0) + G_1(2ml - x, y | x_0, y_0)\} \tag{2.21}$$

or by using (2.19)

$$G(x, y | x_0, y_0) = \sum_{m=-\infty}^{\infty} \sum_{n=0}^{\infty} \frac{\psi_n(y)\psi_n(y_0)}{2k_n d} \{\mathrm{e}^{-k_n|2ml+x-x_0|} + \mathrm{e}^{-k_n|2ml-x-x_0|}\}. \tag{2.22}$$

from which we deduce that

$$G(x, y | x_0, y_0) = \sum_{n=0}^{\infty} \frac{\psi_n(y)\psi_n(y_0)}{2k_n d} \frac{\{\cosh k_n(l - |x - x_0|) + \cosh k_n(l - x - x_0)\}}{\sinh k_n l}. \tag{2.23}$$

We note that G converges everywhere in the domain apart from $(x, y) = (x_0, y_0)$ where it possesses a log singularity.

3. First-order solution

We proceed to find the first order potential using the method of Porter & Porter (2000). We apply Green's Identity

$$\int\int_D (\phi_1 \nabla^2 G - G \nabla^2 \phi_1) \, \mathrm{d}D = \int_S \left(\phi_1 \frac{\partial G}{\partial n} - G \frac{\partial \phi_1}{\partial n} \right) \, \mathrm{d}s$$

where s measures the arc length on S, the boundary of D, which gives

$$-\phi_1(x_0, y_0) = \int_S \left(\phi_1 \frac{\partial G}{\partial n} - G \frac{\partial \phi_1}{\partial n} \right) \, \mathrm{d}s.$$

Now the boundary conditions on G and ϕ_1 mean that the only contribution is from C and therefore

$$\phi_1(x_0, y_0) = -\int_C \phi_1 \frac{\partial G}{\partial n} \, \mathrm{d}s. \tag{3.1}$$

In this form equation (3.1) represents a homogeneous second-kind integral equation for ϕ_1 and hence can be used to determine the sloshing frequencies at first order. We choose to proceed further following Porter & Porter's (2000) technique of converting normal derivatives to tangential derivatives by using the Cauchy-Riemann equations in the form

$$
\begin{aligned}
\frac{\partial}{\partial s}\psi_n(y)\mathrm{e}^{\pm k_n x} &= \mp\frac{\partial}{\partial n}\chi_n(y)\mathrm{e}^{\pm k_n x}, \\
\frac{\partial}{\partial n}\psi_n(y)\mathrm{e}^{\pm k_n x} &= \pm\frac{\partial}{\partial s}\chi_n(y)\mathrm{e}^{\pm k_n x},
\end{aligned}
\tag{3.2}
$$

where

$$
\begin{aligned}
\frac{\partial}{\partial n} &= \frac{1}{\sigma}\left(-h'(x)\frac{\partial}{\partial x}+\frac{\partial}{\partial y}\right), \\
\frac{\partial}{\partial s} &= \frac{1}{\sigma}\left(\frac{\partial}{\partial x}+h'(x)\frac{\partial}{\partial y}\right), \\
\sigma &= \sqrt{(1+(h'(x))^2)}, \\
\chi(y) &= N_n^{-1/2}\sin k_n(d-y).
\end{aligned}
\tag{3.3}
$$

Now using these equations we deduce that

$$
\frac{\partial^2 G}{\partial n\partial n_0} = -\frac{\partial^2 H}{\partial s\partial s_0}
$$

where

$$
H(x,y|x_0,y_0;K) = \sum_{n=0}^{\infty}\frac{\chi_n(y)\chi_n(y_0)}{2k_n d}\frac{\{\cosh k_n(l-|x-x_0|)-\cosh k_n(l-x-x_0)\}}{\sinh k_n l}.
\tag{3.4}
$$

We can now derive an integral equation by differentiating equation (3.1) with respect to n_0 and noting that this derivative must vanish on $y_0 = h(x_0)$. Therefore

$$
\begin{aligned}
0 = \frac{\partial}{\partial n_0}\phi_1(x_0,y_0) &= -\int_C \phi_1(x,y)\frac{\partial^2}{\partial n_0\partial n}G(x_0,y_0|x,y)\,\mathrm{d}s \\
&= \int_C \phi_1(x,y)\frac{\partial^2}{\partial s_0\partial s}H(x_0,y_0|x,y)\,\mathrm{d}s
\end{aligned}
$$

which on integrating with respect to s_0, becomes

$$
C_0 = \int_C \phi_1(x,y)\frac{\partial}{\partial s}H(x_0,y_0|x,y)\,\mathrm{d}s.
$$

We take the limit $x_0 \to l$ where it may be shown from the definition of H that the integrand vanishes and hence C_0, the constant of integration, is zero. We may now integrate by parts to obtain

$$
0 = [\phi_1 H(x_0,h(x_0)|x,y)]_C - \int_C H\frac{\partial\phi_1}{\partial s}\,\mathrm{d}s.
$$

Now it may be easily seen from the definition of $H(x_0,y_0|x,y)$ that the first term above vanishes to give

$$
\int_C H\frac{\partial\phi_1}{\partial s}\,\mathrm{d}s = 0.
\tag{3.5}
$$

If we now define

$$q_1(x) = \left[\frac{\partial \phi_1}{\partial x} + h'(x)\frac{\partial \phi_1}{\partial y}\right]_{y=h(x)} \tag{3.6}$$

and

$$m(x_0, x; K) = \sum_{n=0}^{\infty} \frac{\chi_n(h(x))\chi_n(h(x_0))}{2k_n d} \frac{\{\cosh k_n(l - |x - x_0|) - \cosh k_n(l - x - x_0)\}}{\sinh k_n l}$$
$$\tag{3.7}$$

the integral equation may be rewritten as

$$\int_0^l m(x_0, x; K)q_1(x)\,\mathrm{d}x = 0, \qquad 0 < x_0 < l. \tag{3.8}$$

Non-trivial solutions of this homogeneous first kind integral equation furnish the sloshing frequencies for the tank containing the particular bed shape $y = h(x)$ and the corresponding function $q_1(x)$ which is related to the tangential flux along the bed. In order to solve the second-order problem, however, we must find ϕ_1 in a suitable form to feed into the second-order problem. Specifically this requires the value of ϕ_1 on $y = 0$ so we proceed to find the general form of ϕ_1 everywhere in D and, in particular, its value on the free-surface, $y = 0$.

We now use equations (3.2) to deduce the relation

$$\frac{\partial G}{\partial n} = \frac{\partial L}{\partial s}$$

where $L(x, y|x_0, y_0; K)$ is given by

$$L = \begin{cases} \displaystyle\sum_{n=0}^{\infty} \frac{\chi_n(y)\psi_n(y_0)}{2k_n d}\left\{\frac{\sinh k_n(l - |x - x_0| - \sinh k_n(l - x - x_0)}{\sinh k_n l}\right\}, & x < x_0, \\[4mm] \displaystyle-\sum_{n=0}^{\infty} \frac{\chi_n(y)\psi_n(y_0)}{2k_n d}\left\{\frac{\sinh k_n(l - |x - x_0|) + \sinh k_n(l - x - x_0)}{\sinh k_n l}\right\}, & x > x_0. \end{cases}$$
$$\tag{3.9}$$

Therefore performing integration by parts in equation (3.1) we deduce that

$$\phi_1(x_0, y_0) = -[\phi_1(x, y)L(x, y|x_0, y_0; K)]_C + \int_C L(x, y|x_0, y_0; K)\frac{\partial \phi_1(x, y)}{\partial s}\,\mathrm{d}s. \tag{3.10}$$

A careful treatment of the term $[\phi_1 L]_C$ noting that L is discontinuous at $x = x_0$ yields

$$[\phi L]_C = \phi_1(x_0, h(x_0))\sum_{n=0}^{\infty}\frac{\chi_n(h(x_0))\psi_n(y_0)}{k_n d}. \tag{3.11}$$

This may be simplified using the result

$$\sum_{n=0}^{\infty}\frac{\chi_n(h(x_0))\psi_n(y_0)}{k_n d} = f(y_0) \equiv \begin{cases} 0, & 0 < y_0 < h(x_0), \\ 1, & h(x_0) < y_0 < d \end{cases} \tag{3.12}$$

which is found by expanding the function of y_0 on the right hand side in the complete set $\{\psi_n\}$ to give

$$[\phi_1 L]_C = \phi_1(x_0, h(x_0))f(y_0). \tag{3.13}$$

Finally, upon substituting in equation (3.10) we obtain the expression

$$\phi_1(x_0, y_0) = \int_0^l L(x, h(x)|x_0, y_0; K)q_1(x)\,\mathrm{d}x, \qquad (x_0, y_0) \in D. \tag{3.14}$$

This may be used to find ϕ_1 everywhere in D. However, for our purposes we note that we simply require the expression for ϕ_1 on the undisturbed free-surface $y = 0$. Hence

$$\phi_1(x_0, 0) = \int_0^l L(x, h(x)|x_0, 0; K)q_1(x)\,\mathrm{d}x. \tag{3.15}$$

This result is in terms of the bed-flux function $q_1(x)$ already computed and gives us the all the information we require, both to compute the time-independent first-order wave elevation given by

$$\eta_1(x) = \mathrm{Re}\left\{-\frac{\mathrm{i}\omega}{g}\phi_1(x, 0)\right\},$$

and to feed the first order results into the second-order problem.

4. Second-order solutions

Recall the 2nd order potential Φ_2 must satisfy Laplace's equation together with zero normal derivative on fixed boundaries. Furthermore it must satisfy the complicated free-surface boundary condition (FSBC)

$$\frac{\partial^2 \Phi_2}{\partial t^2} - g\frac{\partial \Phi_2}{\partial y} = \mathrm{Re}[F(x)\mathrm{e}^{-2\mathrm{i}\omega t}] + F_s(x), \qquad \text{on } y = 0$$

as stated in (2.15) and where the terms on the right hand side are defined in equations (2.16) and (2.17). Now, following McIver & McIver (1990), we observe that the right hand side of the FSBC suggests that Φ_2 has the form

$$\Phi_2(x, y, t) = \Phi_s(x, y) - \Gamma t + \mathrm{Re}[\phi_2(x, y)\mathrm{e}^{-2\mathrm{i}\omega t}] \tag{4.1}$$

where the steady and double frequency components of the potential, Φ_s and ϕ_2, both satisfy Laplace's equation and have zero normal derivatives on the fixed boundaries. The FSBC implies the two conditions

$$\frac{\partial \Phi_s}{\partial y} = -\frac{F_s(x)}{g}, \qquad \text{on } y = 0,\ 0 < x < l \tag{4.2}$$

and

$$4K\phi_2 + \frac{\partial \phi_2}{\partial y} = g(x), \qquad \text{on } y = 0,\ 0 < x < l \tag{4.3}$$

where

$$g(x) = -\frac{\mathrm{i}\omega}{g}\left\{\left(\frac{\partial \phi_1}{\partial x}\right)^2 + \frac{3}{2}K^2\phi_1^2 + \frac{1}{2}\phi_1\frac{\partial^2 \phi_1}{\partial x^2}\right\}_{y=0}. \tag{4.4}$$

The choice of Γ simply affects the position of the mean free-surface and is set to a value which guarantees mass conservation, i.e. by requiring no net flux across the undisturbed free-surface. Furthermore, noting that since ϕ_1 satisfies a homogeneous problem, it may be taken to be real without loss of generality, therefore it is evident that $F_s(x) = 0$ in equation (4.2) and consequently Φ_s has zero normal derivative on the boundary $y = 0$.

Then (see, for example, Dettman (1965))

$$\iint_D \nabla\Phi_s.\nabla\Phi_s \, \mathrm{d}D = -\iint_D \Phi_s\nabla^2\Phi_s \, \mathrm{d}D + \int_S \Phi_s\nabla\Phi_s.\mathbf{n} \, \mathrm{d}s = 0.$$

Therefore $\nabla\Phi_s \equiv 0$ in D and so we deduce that Φ_s is a constant which we may set equal to zero without loss of generality.

We now turn to solving for the double frequency component ϕ_2 and we note that $g(x)$ may be calculated in terms of (3.15). The full boundary value problem for ϕ_2 is

$$
\begin{aligned}
\nabla^2\phi_2 &= 0, & (x,y) \in D, \\
\frac{\partial\phi_2}{\partial x} &= 0, & \text{on } \{x = 0,\ 0 < y < h(0)\} \cup \{x = l,\ 0 < y < h(l)\}, \\
4K\phi_2 + \frac{\partial\phi_2}{\partial y} &= g(x), & \text{on } y = 0,\ 0 < x < l, \\
\frac{\partial\phi_2}{\partial n} &= 0, & \text{on } y = h(x),\ 0 < x < l.
\end{aligned}
\tag{4.5}
$$

We proceed to solve for ϕ_2 using the same techniques applied at first-order, but now use the Green's function G given by (2.23) for a frequency of $4K$. So, applying Green's identity, but this time to $\phi_2(x,y)$ and $G(x,y|x_0,y_0;4K)$, gives contributions from the free surface and the bed only. Thus

$$-\phi_2(x_0,y_0) = \int_{y=0} -\phi_2\frac{\partial}{\partial y}G(4K) + G(4K)\frac{\partial\phi_2}{\partial y} \, \mathrm{d}x + \int_C \phi_2(x,y)\frac{\partial}{\partial n}G(4K) \, \mathrm{d}s. \tag{4.6}$$

We now apply the FSBC to obtain

$$-\phi_2(x_0,y_0) = \int_0^l G(x,0|x_0,y_0;4K)g(x) \, \mathrm{d}x + \int_C \phi_2(x,y)\frac{\partial}{\partial n}G(4K) \, \mathrm{d}s. \tag{4.7}$$

In order to proceed as before we need the result

$$\frac{\partial}{\partial n_0}G(x,y|x_0,y_0;K) = \frac{\partial}{\partial s_0}L(x_0,y_0|x,y;K)$$

which is deduced from equations (3.2) and where $L(K)$ is defined by (3.9). We now differentiate with respect to n_0 to give

$$-\frac{\partial}{\partial n_0}\phi_2(x_0,y_0) = \int_0^l \frac{\partial}{\partial n_0}G(x,0|x_0,y_0;4K)g(x) \, \mathrm{d}x - \int_C \frac{\partial^2}{\partial s\partial s_0}H(4K)\phi_2 \, \mathrm{d}s. \tag{4.8}$$

Then applying the bed condition and converting from normal to tangential derivatives we find

$$0 = \int_0^l \frac{\partial}{\partial s_0}L(x_0,h(x_0)|x,0;4K)g(x) \, \mathrm{d}x - \int_C \phi_2\frac{\partial^2}{\partial s\partial s_0}H(4K) \, \mathrm{d}s \qquad \text{on } y_0 = h(x_0). \tag{4.9}$$

We may now integrate with respect to s_0. So

$$C_0 = \int_0^l L(x_0,h(x_0)|x,0;4K)g(x) \, \mathrm{d}x - \int_C \phi_2\frac{\partial}{\partial s}H(4K) \, \mathrm{d}s \qquad \text{on } y_0 = h(x_0) \tag{4.10}$$

and using the limit $x_0 \to 0$ we deduce that $C_0 = 0$. Integrating the second integral by

parts we find that

$$-\int_0^l L(x_0, h(x_0)|x, 0; 4K)g(x)\mathrm{d}x = -[\phi_2 H(4K)]_C + \int_C H(4K)\frac{\partial\phi_2}{\partial s}\mathrm{d}s \qquad \text{on } y_0 = h(x_0),$$
(4.11)

where, since $H(4K) = 0$ at $x_0 = 0, l$ the first term on the right hand side of the equation vanishes, giving

$$-\int_0^l L(x_0, h(x_0)|x, 0; 4K)g(x)\,\mathrm{d}x = \int_C H(4K)\frac{\partial\phi_2}{\partial s}\,\mathrm{d}s \qquad \text{on } y_0 = h(x_0). \qquad (4.12)$$

Now, defining

$$q_2(x) = \left[\frac{\partial\phi_2}{\partial x} + h'(x)\frac{\partial\phi_2}{\partial y}\right]_{y=h(x)} \qquad (4.13)$$

and using equation (3.7) we may rewrite the integral equation (4.11) as

$$f(x_0) \equiv -\int_0^l L(x_0, h(x_0)|x, 0; 4K)g(x)\,\mathrm{d}x = \int_0^l m(x, x_0; 4K)q_2(x)\,\mathrm{d}x. \qquad (4.14)$$

Once we have solved for $q_2(x)$ we find that the solution for ϕ_2 on the free-surface follows using a similar procedure as used previously in equations (3.9) to (3.15). Thus omitting the details we find

$$\phi_2(x_0, 0) = p(x_0) - \int_0^l L(x, h(x)|x_0, 0; 4K)q_2(x)\,\mathrm{d}x, \qquad (4.15)$$

where

$$p(x_0) \equiv -\int_0^l G(x, 0|x_0, 0; 4K)g(x)\,\mathrm{d}x. \qquad (4.16)$$

Once again, ϕ_2 is given in terms of a bed flux function $q_2(x)$ which we have already computed. Now it may be shown from (2.8) that η_2 may be decomposed as

$$\eta_2 = \eta_{20} + \mathrm{Re}\left\{\eta_{22}\mathrm{e}^{-2i\omega t}\right\}$$

with the time independent expressions η_{20} and η_{22} given by

$$\eta_{20} = -\frac{\Gamma}{g} + \frac{1}{4g}\left\{\left(\frac{\partial\phi_1(x,0)}{\partial x}\right)^2 - K^2(\phi_1(x,0))^2\right\}$$

and

$$\eta_{22} = -\frac{2i\omega}{g}\phi_2(x,0) + \frac{1}{4g}\left\{\left(\frac{\partial\phi_1(x,0)}{\partial x}\right)^2 + 3K^2(\phi_1(x,0))^2\right\}$$

respectively. We set Γ by requiring

$$\int_0^l \eta_{20}(x)\,\mathrm{d}x = 0$$

therefore obtaining

$$\Gamma = \frac{1}{4}\int_0^l \left(\frac{\partial\phi_1(x,0)}{\partial x}\right)^2 - K^2(\phi_1(x,0))^2\,\mathrm{d}x.$$

It may easily be shown directly from the formulation of the governing equations that

$$\int_0^l \eta_{22}(x)\,\mathrm{d}x = 0,$$

thus guaranteeing mass conservation, and providing a useful check for our numerical results.

We note that we have all the information to calculate the second-order potential throughout D, and specifically to calculate the second-order surface elevation. Therefore we have effectively formulated the solution of the sloshing problem for arbitrary bed topographies exactly to second-order.

5. Approximation and Numerical Method

Although our formulation of the problem so far is exact we must resort to numerical techniques to generate results. A discussion of the key steps involved is presented below.

5.1. *Calculation of the bed flux* $q_1(x)$

We solve the integral equation (3.8) numerically by using a Galerkin method where we approximate $q_1(x)$ by

$$q_1 \simeq \widetilde{q_1} \equiv \sum_{n=1}^{N} a_n v_n(x). \tag{5.1}$$

We introduce an operator $\mathcal{M}$ where

$$(\mathcal{M}q_1)(x_0) = \int_0^l m(x, x_0; K) q_1(x) \, \mathrm{d}x$$

and define an associated inner product

$$(q_1, p) = \int_0^l q_1(x) \overline{p(x)} \, \mathrm{d}x.$$

A variational principle equivalent to Galerkin's method is used to approximate the solution of the integral equation and takes the form

$$(\mathcal{M}\widetilde{q_1}, v_m(x)) = 0, \qquad m = 1, \ldots, N.$$

This results in the matrix equation

$$\sum_{n=1}^{N} a_n M_{m,n} \equiv \sum_{n=1}^{N} a_n (\mathcal{M}v_n, v_m) = 0, \quad m = 1, \ldots, N. \tag{5.2}$$

We now choose appropriate trial functions to model $q_1(x)$ the fluid flow along the bed particularly at $x = 0, l$. A local analysis of the fluid flow shows that $q_1(x) \to 0$ as $x \to 0, l$ to give zero normal flux. Therefore we choose

$$v_n(x) = \frac{1}{l} \sin\left(\frac{n\pi x}{l}\right), \tag{5.3}$$

and we construct the matrix M with elements $M_{m,n}$ defined by

$$\int_0^l v_m(x) \int_0^l \sum_{r=0}^{\infty} \frac{\chi_r(h(x))\chi_r(h(y))}{2k_r d} \frac{\{\cosh k_r(l - |x - y|) - \cosh k_r(l - x - y)\}}{\sinh k_r l} v_n(y) \, \mathrm{d}y \, \mathrm{d}x.$$

$$\tag{5.4}$$

We note that the terms in $\cosh k_r(l - x - y)$ are separable, so we define

$$gs_{0n} = \int_0^l \chi_0(h(x)) \frac{\sin k(l/2 - x)}{\sin kl/2} v_n(x)\, \mathrm{d}x,$$

$$gc_{0n} = \int_0^l \chi_0(h(x)) \frac{\cos k(l/2 - x)}{\cos kl/2} v_n(x)\, \mathrm{d}x,$$

$$G^{(0)}_{m,n} = \frac{1}{4kd} \left\{ gs_{0n}gs_{0m} \tan(kl/2) - \frac{gs_{0n}gs_{0m}}{\tan(kl/2)} \right\},$$

$$gs_{rn} = \int_0^l \chi_r(h(x)) \frac{\sinh k_r(l/2 - x)}{\sinh k_r l/2} v_n(x)\, \mathrm{d}x, \qquad r = 1, 2, \ldots$$

$$gc_{rn} = \int_0^l \chi_r(h(x)) \frac{\cosh k_r(l/2 - x)}{\cosh k_r l/2} v_n(x)\, \mathrm{d}x, \qquad r = 1, 2, \ldots$$

$$G^{(r)}_{m,n} = \frac{1}{4k_r d} \left\{ gs_{rn}gs_{rm} \tanh(k_r l/2) - \frac{gs_{rn}gs_{rm}}{\tanh(k_r l/2)} \right\}.$$

We also break the terms in $\cosh k_r(l - |x - y|)$ into

$$w_{m,n} = \frac{1}{2kd} \int_0^l \chi_0(h(x)) v_m(x) \int_0^l \chi_0(h(y)) \frac{\cos k(l - |x - y|)}{\sin kl} v_n(y)\, \mathrm{d}y\, \mathrm{d}x \qquad (5.5)$$

and

$$e_{m,n} = \sum_{r=1}^{\infty} \frac{1}{2k_r d} \int_0^l v_m(x) \chi_r(h(x)) \int_0^l \chi_r(h(y)) v_n(y) \frac{\cosh k_r(l - |x - y|)}{\sinh k_r l}\, \mathrm{d}y\, \mathrm{d}x \qquad (5.6)$$

to give

$$M_{m,n} = G^{(0)}_{m,n} - \sum_{r=1}^{\infty} G^{(r)}_{m,n} + w_{m,n} + e_{m,n}. \qquad (5.7)$$

The only term which presents any computational difficulties is $e_{m,n}$ which contains a logarithmic singularity. Porter & Porter (2000) explain how to deal with this term by subtracting the asymptotic leading order contribution and then identifying it as a log function which may be integrated out explicitly. The sloshing frequency and associated bed-flux were found using a standard bisection approach typically involving 12 bisections and hence calculations of the matrix coefficients, to achieve six significant figure accuracy.

5.2. *Calculation of the first-order potential on* $y = 0$

To calculate the first-order wave elevation and to solve the second-order problem we need an easily calculated expression for $\phi_1(x, 0)$. We obtain this by expanding $\phi_1(x, 0)$ as a Fourier cosine series to remain consistent with (5.3) thus obtaining the expression for the first order potential on the free-surface in a readily computable form

$$\phi_1(x, 0) = \sum_{s=0}^{\infty} b_s \cos(s\pi x/l) \qquad (5.8)$$

where

$$b_s = \frac{\varepsilon_s}{l} \int_0^l \int_0^l L(x, h(x)|x_0, 0; K) q_1(x) \cos(s\pi x_0/l)\, \mathrm{d}x\, \mathrm{d}x_0. \qquad (5.9)$$

Of course, b_0 must be equal to zero to guarantee mass conservation, however, anticipating a more compact means of presenting further results, we leave the summation from $s = 0$ but noting that $b_0 = 0$. Now, using our expression for $q_1(x)$ as calculated above we may insert into equation (5.9) to give

$$b_s = \frac{2}{l^2} \sum_{n=1}^{N} a_n \int_0^l \int_0^l L(x, h(x)|x_0, 0; K) \sin(n\pi x/l) \cos(s\pi x_0/l) \, \mathrm{d}x \, \mathrm{d}x_0. \qquad (5.10)$$

In practice we truncate the cosine series for $\phi_1(x, 0)$ taking no more terms than N, the truncation size for the Galerkin approximation. Now, the Fourier coefficient b_s in the form presented at (5.10) is computationally expensive in that, for each s, there is a sum of double integrals of the discontinuous function L which itself involves a sum. If we define

$$L_{n,s}(K) = \int_0^l \int_0^l L(x, h(x)|x_0, 0; K) \sin\left(\frac{n\pi x}{l}\right) \cos\left(\frac{s\pi x_0}{l}\right) \, \mathrm{d}x \, \mathrm{d}x_0 \qquad (5.11)$$

then the b_s may be constructed from sums of the $L_{n,s}(K)$. We note that within the double integral the discontinuous function $L(x, h(x)|x_0, 0; K)$ is evaluated on the free-surface thereby removing the dependence on the arbitrary function $h(x_0)$ and therefore allowing us to separate in the form

$$L_{n,s}(K) = -\int_0^l \sum_{r=0}^{\infty} \frac{\chi_r(h(x))\psi_r(0)}{2k_r d} \sin\left(\frac{n\pi x}{l}\right) (I_1(x) + I_2(x)) \, \mathrm{d}x \qquad (5.12)$$

where

$$I_1(x) = \int_0^l \frac{\operatorname{sgn}(x - x_0) \sinh k_r(l - |x - x_0|)}{\sinh k_r l} \cos\left(\frac{s\pi x_0}{l}\right) \, \mathrm{d}x_0, \qquad (5.13)$$

$$I_2(x) = \int_0^l \frac{\sinh k_r(l - x - x_0)}{\sinh k_r l} \cos\left(\frac{s\pi x_0}{l}\right) \, \mathrm{d}x_0. \qquad (5.14)$$

Using Gradshteyn & Ryzhik (1965) (§2.671:2) we may integrate these directly to give

$$I_1(x) = \frac{k_r l^2}{k_r^2 l^2 + s^2 \pi^2} \frac{(-1)^s \cosh k_r x - \cosh k_r(l - x)}{\sinh(k_r l)} + 2\frac{s\pi l}{k_r^2 l^2 + s^2 \pi^2} \sin\left(\frac{s\pi x}{l}\right),$$

$$I_2(x) = \frac{k_r l^2}{k_r^2 l^2 + s^2 \pi^2} \frac{\cosh k_r(l - x) - (-1)^s \cosh k_r x}{\sinh(k_r l)}. \qquad (5.15)$$

Finally, simplifying we obtain

$$I_1(x) + I_2(x) = \frac{2s\pi l}{(k_r^2 l^2 + s^2 \pi^2)} \sin\left(\frac{s\pi x}{l}\right) \qquad (5.16)$$

which may be used in equation (5.12) to compute $L_{n,s}(K)$. In practice no further progress may be made analytically with equation (5.12) due to the presence of the $h(x)$ term so it must be computed numerically. This however presents no difficulties for a Gaussian quadrature as the procedure above has reduced the problem to a single integral with smooth integrand. We note from our numerical results that the decrease of b_s is much more rapid than the worst case of $O(s^{-4})$ predicted by Fourier theory and

therefore our evaluation of $\phi_1(x,0)$ is not limited by taking modest truncation sizes in the Galerkin approximation.

5.3. *Calculation of the integrals* $f(x_0)$ *and* $p(x_0)$

The integrals $f(x_0)$ in equation (4.14) and $p(x_0)$ in equation (4.16) as they are currently defined are rather complicated. However, the fact that they are defined on $y = 0$ enables us perform the integration analytically. We are able to do this by simplifying the expression for $g(x)$ using the approach presented in Appendix A. In essence this involves calculating the $g(x)$ as a Fourier cosine series in terms of the Fourier coefficients b_s introduced in equation (5.8). Thus in Appendix A it is shown how we may write

$$g(x) = \sum_{n=0}^{2N} g_n \cos(n\pi x/l). \tag{5.17}$$

Using Gradshteyn & Ryzhik (1965) (§2.671:2-3) it is possible to integrate $f(x_0)$ and $p(x_0)$ to give

$$f(x_0) = \sum_{r=0}^{\infty} \frac{\chi_r(h(x_0))\psi_r(0)}{2k_r d} \cdot f_r(x_0) \tag{5.18}$$

where

$$f_r(x_0) = \sum_{s=0}^{2N} g_s \frac{2l\pi s}{k_r^2 l^2 + \pi^2 s^2} \sin(s\pi x_0/l) \tag{5.19}$$

and

$$p(x_0) = \frac{l^2}{d} \sum_{s=0}^{2N} g_s \left(\sum_{r=0}^{\infty} \frac{\psi_r^2(0)}{(k_r^2 l^2 + \pi^2 s^2)} \right) \cos(s\pi x_0/l). \tag{5.20}$$

5.4. *Calculation of the second-order bed flux* $q_2(x)$

Once again we solve using the Galerkin method to find

$$q_2 \simeq \widetilde{q_2} \equiv \sum_{n=1}^{N} c_n v_n(x) \tag{5.21}$$

where the coefficients c_n are found by solving the matrix equation

$$\sum_{n=1}^{N} c_n M_{m,n}(4K) = f_m \qquad m = 1 \dots N. \tag{5.22}$$

Where we define f_m by

$$f_m = \int_0^l f(x_0) v_m(x_0) \, dx_0 \tag{5.23}$$

and $M_{m,n}(4K)$ is the matrix defined in equation (5.7) but operating at $4K$. The integral in (5.23) must be integrated numerically to form the integral equation, but this is relatively inexpensive. In particular, it is worth noting that our code used the extremely efficient routine for summing a Fourier series in Acton (1997) to both sum quickly, and to avoid oscillatory effects. Solution of this inhomogeneous problem is routine, and typically an order of magnitude quicker than the first-order solution, requiring only one calculation of the matrix coefficients.

5.5. *Calculation of the second-order potential on* $y = 0$

Calculation of the second-order potential on $y = 0$ poses no additional problems to those encountered for the first order potential. Equation (4.15) gives two contributions to ϕ_2

$$\phi_2(x_0, 0) = p(x_0) + d(x_0) \tag{5.24}$$

where

$$d(x_0) = -\int_0^l L(x, h(x)|x_0, 0; 4K)q_2(x)\,\mathrm{d}x. \tag{5.25}$$

We see from the definition of $p(x_0)$ (5.20) that it is already in the form of a Fourier cosine series, and $d(x_0)$ may be evaluated to give a Fourier cosine series exactly as for the $\{b_s\}$ at first-order. Therefore we may add both contributions to give ϕ_2 as a Fourier cosine series with coefficients $\{d_s\}$ for $s = 0, 1, 2 \ldots$.

6. Results

The numerical method for the first-order solution has been checked against several analytic results for its accuracy. The first check is made by comparing the computed sloshing frequencies against the known exact solutions (2.12) for a flat-bed. It was found that our method converged to six significant figures for modest truncation sizes ($N = 8$) of the bed flux approximations. Another check can be made by comparing our results with those of Porter & Porter (2003) who considered scattering by a periodic ripple bed. In their work they showed that the onset of Bragg resonance for the scattering of waves by a smooth periodic bed was governed by frequencies at which sloshing occurs over a single period of the bed contained within solid vertical walls. In our problem, we have considered a more general situation in which the bed shape does not have to belong to a smooth periodic structure. In particular Porter & Porter (2003) produced sloshing frequencies for values of $a/d = \frac{1}{2}$ in the two bed shapes given by the functions

$$h(x) = a + \tfrac{1}{2}(d - a)(1 - \cos(2\pi x/l))$$

and

$$h(x) = d - \tfrac{1}{2}(d - a)(1 - \cos(2\pi x/l)).$$

These functions represent cosine curves with minima of $h(x) = a$ at $x = 0$ and $x = l$ in the former case and at $x = \frac{1}{2}l$ in the latter case. Our results using a truncation parameter of $N = 8$ are $Kl = 3.0739$ and $Kl = 2.9508$ respectively and agree with those of Porter & Porter (2003) to the same accuracy. In figure (6.1) we show, graphically, the variation of sloshing frequencies Kl as a/d is varied between $a/d = \frac{1}{2}$ and unity, which corresponds to the flat-bed solution previously mentioned. In figure (6.1) we also plot, for comparison results using the MMSE which were produced via direct integration using an adaptive-stepsize Runge-Kutta-Fehlberg scheme. It can be seen that, as the bed-shape approaches the flat-bed case, all the results approach the analytic solution. Likewise the exact results agree with Porter & Porter (2003) as $a/d \to 0.5$ to within four significant figures with a truncation size of $N = 8$. They also show the correct monotonic decreasing behaviour as $a/d \to 0$ and as predicted by Fox & Kuttler (1983). It can be seen that for mild-slopes the MMSE produces reasonable accuracy as expected, whereas for moderate slopes the results appear more geometry-sensitive. In particular, by using the MSE, one of the geometries fails to show the correct monotonic decreasing behaviour of the frequency for even moderate slopes. As a further check, we confirmed the
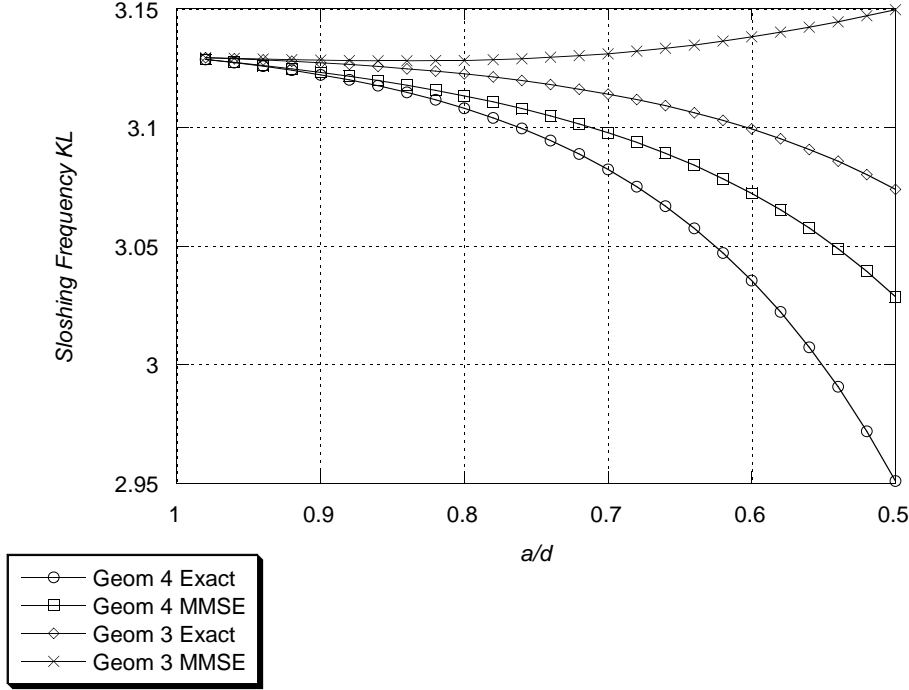
FIGURE 6.1. Sloshing frequencies for the first mode over periodic beds given by (Geom 3 - $h = a + 0.5(d - a)(1 - \cos(2\pi x/l))$) & (Geom 4 - $h = d - 0.5(d - a)(1 - \cos(2\pi x/l))$)

calculations for the MMSE by independently solving via a Green's function formulation giving identical results to those found by direct integration.

We shall adopt the previous notation in what follows by defining a to be the minimum value of $h(x)$ over $0 < x < l$. We proceed for the rest of the paper to consider the two specific geometries in figure (6.2) and for which in the limit $a \to 0$ results are known. Results are presented for domains having various aspect ratios l/d and where a/d is varied in the interval $[0, 1]$. The bed shape for the first geometry is an arc of a circle whose intercept with the vertical walls of the tank at a depth of a defines the radius and in the limit $a \to 0$ (when $l/d = 2$) approaches the semi-circular canal for which results have been computed independently by Evans & Linton (1991) using a semi-analytical method. The second geometry is a canal with a triangular bed which in the limit $a \to 0$ (when $l/d = 2$) approaches the geometry for which Lamb (1932) provides an analytic solution, corresponding to sloshing in a right-angled wedge. Lamb's sloshing frequencies are thus determined by the roots of the equation

$$\tanh kd = \pm \tan kd$$

where $+(-)$ corresponds to antisymmetric(symmetric) modes.

Figure (6.3) shows a graph of the sloshing frequency normalised by dividing by the flat-bed solution (2.14) plotted against a/d for the first sloshing mode over a triangular bed in a tank whose aspect ratio is governed by the relation $l/d = 2\cot(\pi/n)$ for $n = 3, 4, \ldots, 8$. This means that, when $a = 0$, the angle that each section of sloping
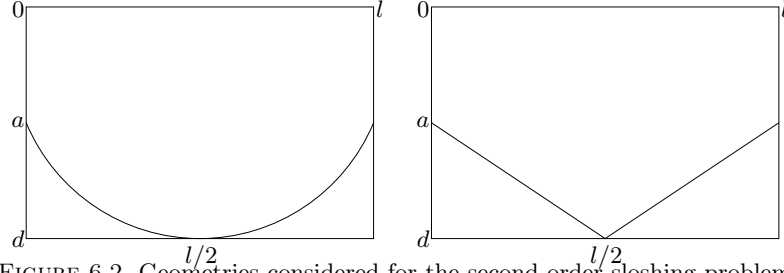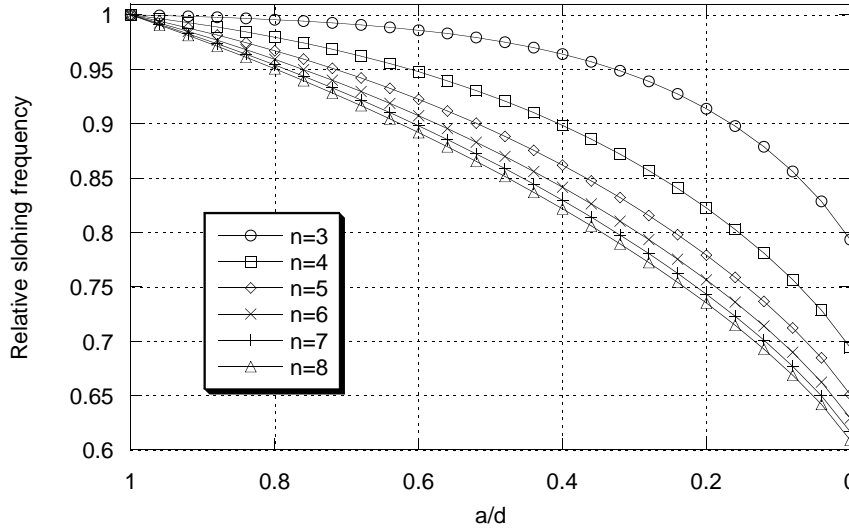
FIGURE 6.2. Geometries considered for the second-order sloshing problem

FIGURE 6.3. Normalised sloshing frequencies for the first mode over a triangular bed making
an angle of π/n with the horizontal bed

bottom makes with the horizontal is π/n. Thus, in figure (6.3), the variation of a/d from one to zero represents the transition from the flat-bed solution to the triangular canal solution. This case was run first with the trial function $\sin(n\pi x/l)$ where we found that in the limits $a/d \to 1$ we obtained the correct results to the required accuracy. In the limit $a/d \to 0$ we obtained the results given by Lamb (1932) for the bed of slope $\pi/4$ accurate to four significant figures ($Kl = 1.000$). Then, noting that the first mode is antisymmetric, we anticipated a bed-flux symmetric around $l/2$ and therefore ran the code again choosing $\sin((2n-1)\pi x/l)$ as the trial function. The latter results are presented because, as expected, they give slightly better convergence for fixed maximum truncation size. Results over the same bed shapes are also presented at figure (6.4) for the second mode which is symmetric and therefore requires the trial function $\sin(2n\pi x/l)$. In this case we are able to verify that, in the limit $a/d \to 0$, the results for the bed of slope $\pi/6$ agree with analytic results in Lamb (1932) and Packham (1980) in which $Kl = 3.464$.

Figure 6.5 shows a graph of the non-dimensional frequency Kl against a/d for the first mode over a symmetric bed in the shape of an arc of a circle and where the tank aspect ratio is $l/d = 2$. The results are bounded from above by the rectangular canal solution and from below by the semi-circular canal solution which has also been computed by Evans & Linton (1991) as $Kl = 2.7114$. This case was run first with the trial function
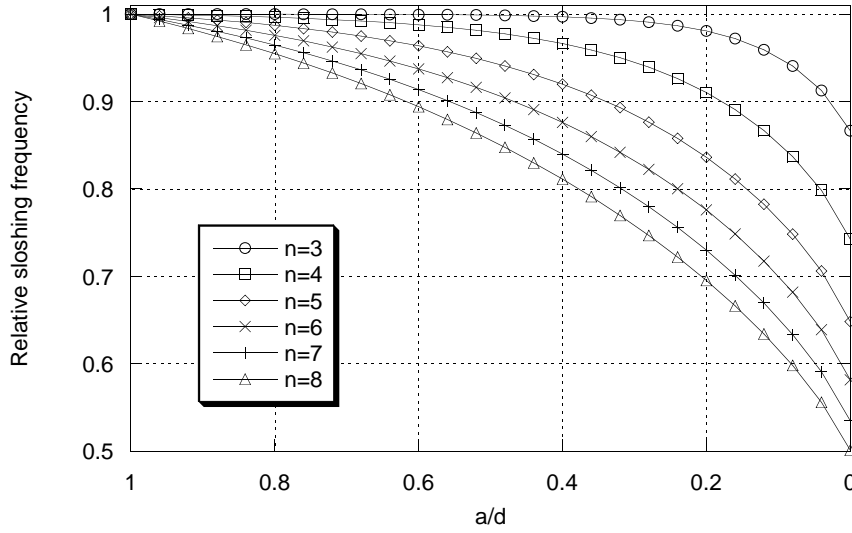
FIGURE 6.4. Normalised sloshing frequencies for the second mode over a triangular bed making an angle of π/n with the horizontal
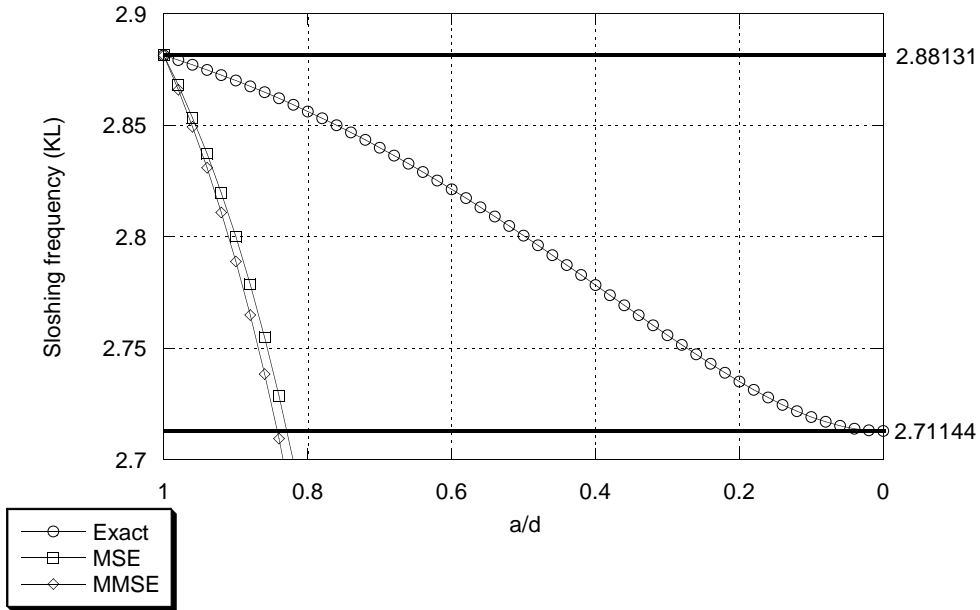

FIGURE 6.5. Sloshing frequencies for the first mode over an arced bed

$\sin(n\pi x/l)$ where we found that, in the limits $a/d \to 1$ and $a/d \to 0$ we obtained the correct results. Again we re-ran the code anticipating a bed flux symmetric around $l/2$ using $\sin((2n-1)\pi x/l)$ as the trial function and we present the latter results. Alongside we provide, for comparison, equivalent results using the MMSE. Surprisingly in this case the accuracy of the MMSE results is extremely poor even for mild slopes.

For the flat-bed case $a/d = 1$ all of our results were found to agree with the analytical results to six significant figures with modest truncation sizes ($N = 8$). For the limit $a \to$

a/d	$N=6$	$N=12$	$N=18$	$N=24$	$N=30$	$N=36$	$N=42$	$N=48$
1.00	1.44066	-	-	-	-	-	-	-
0.90	1.42759	-	-	-	-	-	-	-
0.80	1.41125	1.41124	-	-	-	-	-	-
0.70	1.39083	1.39082	-	-	-	-	-	-
0.60	1.36537	1.36535	-	-	-	-	-	-
0.50	1.33372	1.33369	-	-	-	-	-	-
0.40	1.29445	1.29441	1.29440	-	-	-	-	-
0.30	1.24579	1.24569	1.24568	-	-	-	-	-
0.20	1.18525	1.18504	1.18502	1.18501	-	-	-	-
0.10	1.10859	1.10810	1.10804	1.10803	1.10802	-	-	-
0.05	1.06134	1.06043	1.06032	1.06029	1.06028	1.06027	-	-
0.00	1.00367	1.00094	1.00042	1.00024	1.00015	1.00010	1.00007	1.00006

TABLE 6.1. Convergence of results for sloshing frequency K

0 we obtained four significant figure accuracy against known results for the triangular bed shape and three significant figures for the semi-circular bed shape using the $\sin(n\pi x/l)$ trial function and using a truncation size of ($N = 48$). Using Legendre functions we were able to obtain six significant figure accuracy for the first symmetric mode in the triangular canal problem where $l/d = 2$. It is to be expected that our approach will cause problems when $a = 0$ as, at this point the bed meets the free-surface. This problem manifests itself in our assumptions about the local behaviour of the fluid flow at the join with the canal walls. In the case of the semi-circular bed the condition at the end of the bed remains zero flux however this is inconsistent with the free-surface condition at this point. In the triangular case the Legendre function was chosen to model the high fluxes anticipated in the region thus apparently improving the local modelling and regaining the required accuracy. We found that, in order to improve on these results we needed to take more terms in the Fourier series expansion and even then found weak convergence as expected with a Fourier series representation in this case.

Table (6.1) shows how convergence for the first mode of the triangular bed depends upon the truncation size. We use a dash to denote no further improvement in results. It is clearly seen that the Galerkin approach provides efficient convergence reaching at least four significant figures for a truncation size of $(N = 12)$. In fact it is only the extreme case where $a/d \approx 0$ that increased truncation size is required to account for the problems we anticipate at that limit in this formulation, nevertheless we see that four significant figures are still obtained for a modest $N = 12$.

We move now to the results for the second-order problem where it can be shown that the analytical solution for the forced double-frequency term at second-order for a flat-bottomed tank corresponding to the n th first-order mode of

$$\phi_1 = \frac{gA \cos \mu_n x \cosh \mu_n (y - d)}{\omega \cosh \mu_n d}$$

where $K = \omega_n^2/g$, is given by

$$\phi_2 = \frac{-\mathrm{i}A^2 \sqrt{g}(3K^2 + \mu_n^2)}{16\sqrt{K^3}} + \frac{-\mathrm{i}3A^2 \sqrt{g}(K^4 - \mu_n^4) \cos 2\mu_n x \cosh 2\mu_n (y - d)}{16\sqrt{K^7} \cosh 2\mu_n d}. \qquad (6.1)$$

The expression for ϕ_2 is easily derived following the formulation of the problem in this

n	a_n	b_n	ic_n	id_n
0				0.988842
1	0.925275	2.67999	0	0
2	0	0	0.531020	-0.493030
3	0.368583	0.011046	0	0
4	0	0	0.205348	0.142988
5	0.012162	0.000303	0	0
6	0	0	0.040089	0.002149
7	0.080727	0.000019	0	0
8	0	0	0.039160	0.000132
9	0.002728	0.000001	0	0
10	0	0	0.018101	0.000010
11	0.036602	0	0	0
12	0	0	0.018440	0

TABLE 6.2. Table of results for second-order sloshing over a triangular bed where $a/d = 0.6$, $N = 12$ and $Kl = 2.73073$

paper. For an alternative derivation in the time domain, see Wu & Eatock Taylor (1994) who use this result to calibrate their finite-element analysis code. However, it should be noted that the second term in the expression above differs slightly from that presented in the reference which appears dimensionally incorrect. Our code was run with a Fourier series truncation size of 10 to find the first sloshing frequency to six significant figure accuracy. We found full agreement with the second-order analytic solution in (6.1), to five significant figures. In particular we found that in the limit $a \to 1$, the contribution to ϕ_2 came from $p(x_0)$. However, as we decreased a we found that the contribution from $d(x)$ grew such that we still obtained agreement with (6.1) to five significant figures.

We now solve the full second-order problem for second-order sloshing over a triangular bed. Table (6.2) displays the results for the case where $a/d = 0.6$ for a truncation size of $N = 12$. It can be shown from our formulation that Mass conservation is guaranteed using the infinite Fourier series representation of the first-order potential on the free-surface. Therefore calculation of the integral of η_{22} over the free-surface provides a valuable measure of the error introduced in truncating the Fourier series. In this case we find that the integral of η_{22} over the surface is 3×10^{-6} which implies that we have retained the 5 significant figure accuracy we obtained for the flat bed with this truncation size. Figure (6.6) plots snapshots of both the first-order and second-order surface elevations (η_1 and η_2 respectively) at regular intervals in half a period of oscillation for the case where $a/d = 0.5$ and for the same truncation size $N = 12$. In this case we find that the integral of η_{22} over the surface is 7×10^{-6}. The second half of the period is simply the same sequence of snapshots with η_1 replaced by $-\eta_1$. We normalised the first mode of the free surface potential to give a first-order surface elevation of unit amplitude in order to compare all other contributions with this dominant mode. In order to construct the total surface elevation including both the first and second-order terms we use $\eta = \varepsilon\eta_1 + \varepsilon^2\eta_2$ where ε represents the wave steepness.

The major computational effort is in finding the sloshing frequency via a bisection method where each step involves a calculation of the matrix in (5.7). There is significant code reuse provided the matrix equation is coded with frequency as a parameter, in which case to solve the second-order problem we only need calculate the matrix once
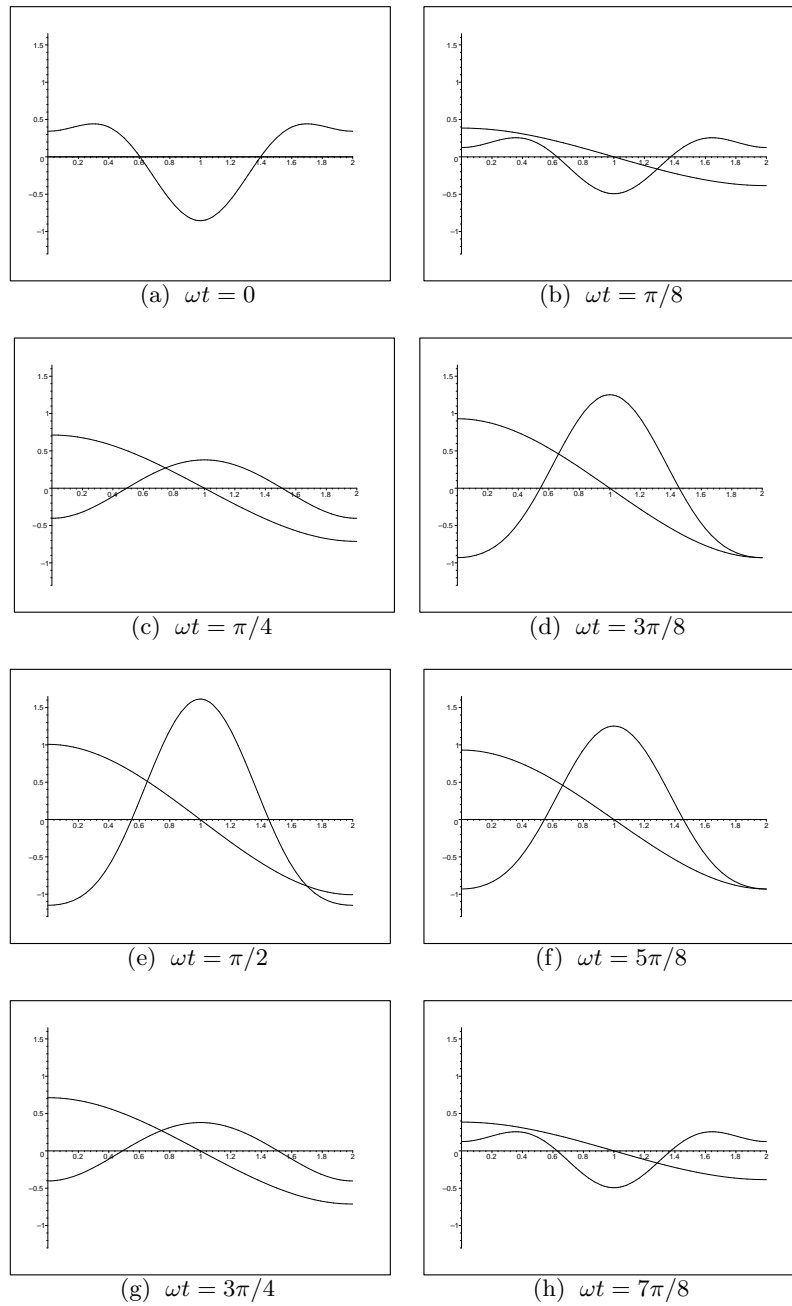
FIGURE 6.6. First-Order ($\sim \cos(\pi x/l)$) and Second-order wave elevations for sloshing over a triangular bed $(a/d) = 0.5$

more using a frequency twice the first-order sloshing frequency. We observe that, once the linear sloshing problem is solved for the bed shape under consideration, the second-order problem may be solved relatively easily with our approach.

7. Conclusions

In a weakly non-linear model of wave problems, in order to produce reliable results at second (and higher) orders, extremely accurate solutions are required at the lower orders. This paper has shown how to provide a lower order(linear) solution for a complicated geometry and feed it into the next higher order of approximation retaining an exact formulation with regards both to the bed condition and the free-surface condition. This approach may be extended to higher orders giving the possibility of highly accurate representations although it is noted that the calculation of the free-surface coefficients becomes increasingly more complicated as the order increases. The solutions are shown to converge rapidly requiring quite modest truncations of the series representations of the solutions.

Although useful in its own rights and offering a practical means of investigating second-order effects, it is envisaged that this method will provide a valuable means of testing fully non-linear solvers. It will enable them to be calibrated against a weakly non-linear model of motion over more realistic geometries. The method of solution can be extended, for example, to higher orders in the Stokes expansion and also to the situation where the tank is forced to oscillate at a frequency both away from, and near to, resonance a problem which is currently being investigated.

Appendix A. Calculation of $g(x)$

We note that $g(x)$ depends on products of the first-order potential on the free surface and its derivatives which we have found as a finite Fourier series as below

$$\phi_1(x,0) = \sum_{n=1}^{N} b_n \cos(n\pi x/l).$$

Therefore treating each component of $g(x)$ separately we have

$$\phi_1^2 = \sum_{n=1}^{N} \sum_{m=1}^{N} b_n b_m \cos \mu_n x \cos \mu_m x$$

$$= \frac{1}{2} \sum_{n=1}^{N} \sum_{m=1}^{N} b_n b_m (\cos \mu_{n+m} x + \cos \mu_{n-m} x).$$

Also

$$\left(\frac{\partial \phi_1}{\partial x}\right)^2 = \sum_{n=1}^{N} \sum_{m=1}^{N} \mu_n \mu_m b_n b_m \sin \mu_n x \sin \mu_m x$$

$$= \frac{1}{2} \sum_{n=1}^{N} \sum_{m=1}^{N} \mu_n \mu_m b_n b_m (\cos \mu_{n-m} x - \cos \mu_{n+m} x),$$

and

$$\phi_1 \frac{\partial^2 \phi_1}{\partial x^2} = - \left(\sum_{n=1}^{N} b_n \cos \mu_n x \right) \left(\sum_{m=1}^{N} \mu_m^2 b_m \cos \mu_m x \right)$$

$$= -\frac{1}{2} \left(\sum_{n=1}^{N} \sum_{m=1}^{N} b_n b_m \mu_m^2 (\cos \mu_{m+n} x + \cos \mu_{n-m} x) \right).$$

Combining the above three results, converting to finite sums and simplifying we find that

$$\frac{g(x)}{-i\omega/g} = \frac{1}{4} \sum_{n=1}^{N} \sum_{m=1}^{N} b_n b_m (3K^2 + 2\mu_n \mu_m - \mu_m^2) \cos \mu_{n-m} x$$

$$+\frac{1}{4} \sum_{n=1}^{N} \sum_{m=1}^{N} b_n b_m (3K^2 - 2\mu_n \mu_m - \mu_m^2) \cos \mu_{n+m} x$$

Now we seek to write

$$g(x) = \sum_{s=0}^{2N} g_s \cos(s\pi x/l) \tag{A.1}$$

where the limits reflect that terms in μ_{n-m} contribute for $s = 0 \ldots N-1$ and the terms in μ_{n+m} contribute for $s = 2 \ldots 2N$. After some algebra it may be seen that the four distinct contributions to the Fourier series for $g(x)$ simplify to give

$$\frac{g(x)}{-i\omega/g} = \frac{1}{4} \sum_{n=1}^{N} b_n^2 (3K^2 + \mu_n^2),$$

$$+ \frac{1}{4} \sum_{s=1}^{N-1} \sum_{n=s+1}^{N} b_{n-s} b_n (6K^2 + 2\mu_n \mu_{n-s} - \mu_s^2) \cos \mu_s x$$

$$+ \frac{1}{4} \sum_{s=2}^{N+1} \sum_{n=1}^{s-1} b_{s-n} b_n (3K^2 - \mu_{s-n}(2\mu_n + \mu_{s-n})) \cos \mu_s x$$

$$+ \frac{1}{4} \sum_{s=N+2}^{2N} \sum_{n=s-N}^{N} b_{s-n} b_n (3K^2 - \mu_{s-n}(2\mu_n + \mu_{s-n})) \cos \mu_s x$$

This expansion has been extensively verified using Mathematica for a wide range of values of b_n. The coefficients of this series are extremely easy to calculate and give us a much easier form of $g(x)$ to deal with.

REFERENCES

ACTON, F. 1997 *Numerical methods that work.* The Mathematical Association of America.

BELIBASSAKIS, K. A. & ATHANASSOULIS, G. A. 2002 Extension of second-order Stokes theory to variable bathymetry. *J. Fluid Mech.* **464**, 35–80.

BERKHOFF, J. C. W. 1973 Computation of combined refraction-diffraction. *Proc. 13th Intl Conf. on Coastal Engng, July 1972, Vancouver Canada.*, 471–490.

BOOIJ, N. 1983 A note on the accuracy of the mild-slope equation. *Coastal Engineering* **7**, 191–203.

CHAMBERLAIN, P. G. & PORTER, D. 1995 The modified mild-slope equation. *J. Fluid Mech.* **291**, 393–407.

CRAGGS, J. W. & DUCK, P. W. 1978 A power series method for treating mixed boundary value problems. *J. Inst. Maths Applics.* **21**, 1–12.

DAVIS, A. M. J. 1965 Two dimensional oscillations in a canal of arbitrary cross section. *Proc. Camb. Phil. Soc.* **61**(1) 827–846.

DAVIS, A. M. J. 1974 Short surface waves in a canal; dependence of frequency on the curvatures and their derivatives. *Q. Jl Mech. appl. Math.* **27**(1) 523–535.

DETTMAN, J. W. 1965 *Applied Complex Variables.* Dover.

EVANS, D. V. & LINTON, C. M. 1991 Sloshing frequencies *Q. Jl Mech. appl. Math.* **46**(1) 71–87.

FALTINSEN, O. M. 1974 A Nonlinear theory of sloshing in rectangular tanks. *Journal of Ship Research* **Vol 18, No 4**, 224-241.

FALTINSEN, O. M. & ROGNEBAKKE, O. V. & LUKOVSKY, I. A. & TIMOKHA, A. N. 2000 Multidimensional modal analysis of nonlinear sloshing in a rectangular tank with finite water depth. *J. Fluid Mech.* 407, 201–234.

FALTINSEN, O. M. & TIMOKHA, A. N. 2001 An adaptive multimodal approach to nonlinear sloshing in a rectangular tank. *J. Fluid Mech.* **432**, 167–200.

FALTINSEN, O. M. & TIMOKHA, A. N. 2002 Asymptotic modal approximation of nonlinear resonant sloshing in a rectangular tank with small fluid depth. *J. Fluid Mech.* **470**, 319–357.

FALTINSEN, O. M. ROGNEBAKKE, O. F. & TIMOKHA, A. N. 2002 Resonant three-dimensional nonlinear sloshing in a square base basin. *J. Fluid Mech.* **487**, 1–42.

FOX, D. W. & KUTTLER, J. R. 1983 Sloshing frequencies *Z. angew. Math. Phys.* **34**, 668–696.

GRADSHTEYN, I. S. & RYZHIK I. M. 1965 *Table of Integrals, Series and Products.* Academic Press.

HENRICI, P. TROESCH, B. A. & WUYTACK, L. 1970 Sloshing frequencies for a half-space with circular or strip-like aperture *Z. angew. Math. Phys.* **21**, 285–318.

LAMB, H. 1932 *Hydrodynamics (6th ed)* Cambridge University Press.

MCIVER, P. 1989 Sloshing frequencies for cylindrical and spherical containers filled to an arbitrary depth. *J. Fluid Mech.* **201**, 243–257.

MCIVER, M. 1994 Second-order wave diffraction in two dimensions. *Applied Ocean Research* **16**, 19–25.

MCIVER, M. & MCIVER, P. 1990 Second-order wave diffraction by a submerged circular cylinder. *J. Fluid Mech.* **219**, 519–529.

MALENICA, Š, EATOCK TAYLOR, R & HUANG, J.B. 1999 Second-order water wave diffraction by an array of vertical cylinders. *J. Fluid Mech.* **390**, 349–373.

MEI, C. C. 1983 *The applied dynamics of ocean surface waves.* Wiley-Interscience.

MILES, J. W. 1972 On the eigenvalue problem for fluid sloshing in a half-space *Z. angew. Math. Phys.* **23**, 861–869.

MOISEEV, N. N. 1964 Introduction to the theory of oscillations of liquid-containing bodies *Advances in Appl. Mech.* **8**, 233–289.

MOISEEV, N. N. & PETROV, A. A. 1968 The calculation of free oscillations of a liquid in a motionless container *Advances in Appl. Mech.* **9**, 91–154.

NADAOKA, K. & BEJI, S. & NAKAGAWA, Y. 1997 A fully dispersive weakly non-linear model for water waves. *Proc. R. Soc. Lond. A.* **453**, 303–319.

PACKHAM, B. A. 1980 Small-amplitude waves in a straight channel of uniform triangular cross-section. *Quart. J. Mech. Appl. Math.* **33**, 179–187.

PORTER, R. & PORTER, D. 2000 Water wave scattering by a step of arbitrary profile. *J. Fluid Mech.* **411**, 131–164.

PORTER, R. & PORTER, D. 2003 Scattered and free waves over periodic beds. *J. Fluid Mech.* **489**, 129–163.

RHEE, J. P. 1997 On the transmission of water waves over a shelf. *Applied Ocean Research* **23**, 299–304.

RHEE, J. P. 2001 A note on the diffraction of obliquely incident water waves by a stepwise obstacle. *Applied Ocean Research* **23**, 299–304.

SOLAAS, F. & FALTINSEN, O. M. 1997 Combined numerical and analytical solution for sloshing in two-dimensional tanks of a general shape. *Journal of Ship Research.* **41**, 118–129.

STOKES, G. G. 1847 On the theory of oscillatory waves. *Camb. Trans.* **1847 Vol 8**, 441–455.

TROESCH, B. A. & TROESCH, H. R. 1972 A remark on the sloshing frequencies for a half-space. *Z. angew. Math. Phys.* **23**, 703–711.

TROESCH, B. A. 1973 Sloshing frequencies in a half-space by Kelvin inversion. *Pacific.J. Math.* **47**, 539–552.

TROESCH, B. A. 1972 Proof of a conjecture on sloshing frequencies in a half-space. *Z. angew. Math. Phys.* **25**, 655–657.

VADA, T. 1987 A numerical solution of the second-order wave-diffraction problem for a submerged cylinder of arbitrary shape. *J. Fluid Mech.* **174**, 23–37.

WU, G. X. & EATOCK TAYLOR, R. 1994 Finite element analysis of two-dimensional non-linear transient water waves. *Applied Ocean Research* **16**, 363–372.

WU, G. X. & EATOCK TAYLOR, R. 1998 Numerical simulation of sloshing waves in a 3D tank based on a finite element method. *Applied Ocean Research* **20**, 337–356.

WEHAUSEN, J.V. & LAITONE, E.V. 1960 *Surface Waves.* Online Edition.